Journal of Alloys and Compounds 683 (2016) 292–301

Contents lists available at ScienceDirect

Journal of Alloys and Compounds

journal homepage: http://www.elsevier.com/locate/jalcom

Nitrogen incorporation and composition facilitated tailoring of the optical constants and dispersion energy parameters of tungsten oxynitride films

O.R. Nunez [a], A.J. Moreno Tarango [a], N.R. Murphy [b], C.V. Ramana [a, *]

[a] Department of Mechanical Engineering, University of Texas at El Paso, El Paso, TX 79968, USA
[b] Materials and Manufacturing Directorate (RX), 3005 Hobson Way, Wright-Patterson Air Force Base (WPAFB), Dayton, OH 45433, USA

ARTICLE INFO

Article history:
Received 20 January 2016
Received in revised form
16 April 2016
Accepted 18 April 2016
Available online 20 April 2016

Keywords:
Tungsten oxynitride
Thin films
Optical constants
Ellipsometry

ABSTRACT

Optical properties, including the index of refraction, extinction coefficient and band gap of 100 nm thick tungsten oxynitride (W-O-N) films are reported. In addition, the Wemple and DiDomenico (WDD) model was used to calculate the dispersion energies and oscillator energies of the films, establishing a correlation among the films' optical, chemical, and physical properties, as a function of nitrogen content. Nitrogen concentration in the W-O-N films was varied by adjusting the nitrogen gas flow rate from 0 to 20 sccm while keeping total gas flow (nitrogen + oxygen + argon) constant at 40 sccm. Both the index of refraction (n) and extinction coefficient (k) of W-O-N films demonstrated a high degree of sensitivity to the nitrogen content during deposition. The optical constants of films fabricated without any nitrogen correspond to transparent W-oxide (WO_3) where $n_{550} = 2.1$ and $k_{550} = 0.0$. The magnitude of the spectral response for both n and k tends to increase with increasing nitrogen content. Systematic increases of the films' nitrogen content lead to the formation of W-oxide ($E_g \approx 3$ eV) → W-O-N oxynitride semiconductor ($E_g \approx 2$ eV) → N-rich W-O-N semi-metal ($E_g < 2$ eV) → WN_2 type metallic transition was evident in dispersion profiles of n and k for W-O-N films with increasing nitrogen content. The corresponding mechanical characteristics, namely hardness (H) and Young's modulus (E), attain a maximum of 4.46 GPa and 98.5 GPa, respectively, at a nitrogen flow rate of 5 sccm, at which point H and E values decrease to attain 3.57 GPa and 72.91 GPa, respectively. The trend observed in H and E values correlate with the W-O and W-N bonds formation in W-O-N along with the interruption of local epitaxy attributed to increasing nitrogen content within the growth chamber. A correlation among the nitrogen content, optical constants and physical properties, along with the associated dispersion model, is presented to account for the optical properties of sputter-deposited W-O-N films. The results demonstrate that tailoring the properties of W-O-N films for desired applications can be achieved by tuning the nitrogen content and chemical composition.

© 2016 Published by Elsevier B.V.

1. Introduction

Optical and electro-optic (EO) thin films and devices based on transition metal oxynitrides, which combine the mechanical properties of transition metal nitrides with the optical and electrical properties of their counterpart metal oxides, are gaining remarkable recent interest. The oxynitride family of materials, which can be represented chemically by MO_xN_y or M-O-N, can offer advantages over the nitride-oxide end members, provide ability to tune the desired properties based on the chemical composition. In addition, oxynitrides can combine the traditional advantages of oxides and nitrides, such as high hardness, oxidation resistance and structural stability at elevated temperatures.

Tungsten oxide (WO_3) is an n-type semiconductor, which exhibits attractive physical, chemical and electronic properties for application in numerous scientific and technological applications in the fields of optics, photovoltaics and optoelectronics [1–10]. WO_3 is commonly referred to as a "chromogenic material" in view of its coloration properties under variable physical and chemical conditions [1–4]. The favorable optical properties described make WO_3 an interesting material, specifically for optics, photovoltaics and

* Corresponding author.
E-mail address: rvchintalapalle@utep.edu (C.V. Ramana).

http://dx.doi.org/10.1016/j.jallcom.2016.04.182
0925-8388/© 2016 Published by Elsevier B.V.

optoelectronics [1–10]. For instance, WO_3 thin films are often applied in display devices due to their ability to perform oxidation state alterations by field-aided ion intercalation [1–4]. Furthermore, the electronic structure of WO_3 films and nanostructures allow the efficient use of the solar spectrum including absorption in the blue part of the visible region and the ultraviolet region, as well as a high transmission region that extends from the near-infrared (IR) to the visible spectrum [1–4]. When these properties are combined with good charge-transport characteristics, photosensitivity, and chemical integrity, WO_3-based materials are attractive for applications related to sustainable energy production including energy efficient windows and architecture, photoelectrochemical water-splitting, photocatalysis and solar cells [1–11]. However, WO_3 exhibits absorption in the near ultraviolet and blue regions of the solar spectrum [12–14]. Tuning the band gap of WO_3 is, therefore, critical to extend the absorption to the longer wavelengths in order to increase the photo-electrochemical performance for water splitting by reducing charge recombination and enhanced light absorption [9,14]. One method that has shown significant promise for tuning the band gap of various is the incorporation of nitrogen, which has demonstrated significant effects on the electronic structure of constituent materials. For instance, there were numerous efforts on nitrogen (N) doping into TiO_2 and ZnO illustrating the electronic structure changes [15–20]. Furthermore, efforts directed at doping anions into TiO_2, the very first successful photo-anode, to improve the photoresponse, have proven that N-doping is the most promising approach [15–21]. However, experiments exploring the fabrication and characterization of tungsten oxynitrides (W-O-N) are not as common as Ti-O-N or N-doped ZnO [15–21]. Specifically, while there are some overall efforts on the effect of N-doping on the microstructure, studies focused on the comprehensive understanding of the optical parameters and their dependence on the effective nitrogen content, and the associated electronic structure changes, are scarce. On the other hand, such studies proved to be valuable in deriving a comprehensive understanding of the electronic properties and photochemical performance of Ti- and Zn-based materials. The present work was, therefore, performed on reactively sputter-deposited tungsten oxynitride films. Reactive sputtering enables the user to fabricate high quality films with a large degree of control of chemical composition, structure and thickness, depending on the deposition parameters chosen. Reactive sputtering is also known to improve mechanical properties of transition metal nitride thin films by enabling nitrogen to react with metal to form the metal nitride films.

The objective of the present work is to derive a comprehensive understanding of the optical constants and dispersion energy parameters of W-O-N films with varying nitrogen content. Determination of the optical properties, specifically the index of refraction (n), extinction coefficient (k) and band gap, for oxides and oxynitrides is not only important to study their fundamental optical properties but also to tailor their electrical conductivity to best suit the given practical applications. However, for thin films and nanomaterials, the optical constants and their dispersion profiles are highly sensitive to structure and composition. Optical properties are influenced by various factors such as chemical composition, surface and interface morphologies, crystal structure, packing density, lattice parameters, and defect structure. Therefore, understanding the optical properties of W-O-N, as a function of processing conditions, allows the user to tailor the spectral dispersion of both n and k, providing a road-map for engineering modern electronic and optical devices such as organic solar cells, electro-optic sensors, and optical transistors. In order to investigate the relationship between nitrogen content and optical performance in the W-O-N material system, spectroscopic ellipsometry (SE) has been employed to measure the optical properties of sputter-deposited W-O-N films. SE is a non-destructive method and provides a detailed account of the optical properties of thin films and coatings. The mechanical properties of W-O-N films were also investigated in order to evaluate their hardness and Young's modulus as a function of processing parameters. As presented and discussed in this paper, the results demonstrate that the optical and mechanical properties of W-O-N films can be tailored by tuning the processing conditions.

2. Experimental

W-O-N films were deposited onto clean silicon (Si) (100) substrates by direct current (DC) sputtering. Silicon substrates were cleaned by RCA (Radio Corporation of America) cleaning and were dried before introducing into the vacuum chamber, which had been evacuated to a base pressure of ~3×10^{-7} Torr. A Tungsten (W) target (Plasmaterials Inc.) of 50 mm diameter and 99.95% purity was employed for reactive sputtering. DC power was supplied to the W-target by an Advanced Energy MDX 500 DC power supply with the sputter source at a distance of 80 mm from the substrates. Once an adequate base pressure was reached, 20 sccm of argon was introduced into the chamber and the plasma was ignited at a power of 100 W. For reactive deposition, and to fabricate W-O-N films, oxygen (O_2) and nitrogen (N_2) were employed alongside argon (Ar). The total gas flow was kept constant at 40 sccm, resulting in a working pressure of 10 mTorr at a pumping speed of 50 L/s. While Ar flow was maintained constant at 20 sccm, the net O_2 and N_2 gas flow rates were adjusted to a total of 20 sccm. The effect of the ratio of nitrogen to oxygen was varied in order to understand the effect of nitrogen content on the mechanical and optical properties of W-O-N films. Before each deposition, the target was pre-sputtered for 10 min in Ar with the gun shutter closed. The depositions were carried out at room temperature (25 °C) for a time period sufficient to reach a film thickness of ≈100 nm.

Optical properties were evaluated using spectrophotometric and ellipsometry measurements. Spectroscopic ellipsometry (SE) was performed ex-situ on the films grown on silicon wafers using a J. A. Woollam α-SE instrument. Measurements were done in the range of 381–900 nm with a step size of 2 nm and at angles of incidence of 65°, 70°, and 75°, near the Brewster's angle of silicon. The ellipsometry data analysis was performed using commercially available CompleteEase software [22]. Films grown on optical grade quartz were employed for optical property measurements to probe the transparent nature and band gap of the W-O-N films. Spectrophotometry measurements were made using a Cary 5000 UV-VIS-NR double-beam spectrophotometer.

Mechanical properties, hardness and reduced elastic modulus, of W-O-N films deposited on Si (100) substrates were measured using a traditional nano-indentation method. Load control nano-indentation was performed using a Hysitron TI 750 TriboIndenter employing a Berkovich tip with a 396 nm radius of curvature. Loading and unloading curves were produced by using a maximum load value of 100 μN, which allowed a shallow penetration depth of the W-O-N between 10 nm and 20 nm, depending on the hardness of each respective sample. In order to obtain reliable information and best possible values of mechanical characteristics, 12 indentations were performed on each sample and the results were averaged to a single set of data.

3. Results and discussion

The representative XRD patterns obtained for W-O-N films deposited under variable nitrogen gas flow rate are shown in Fig. 1. All the films exhibit diffuse patterns, the characteristic of

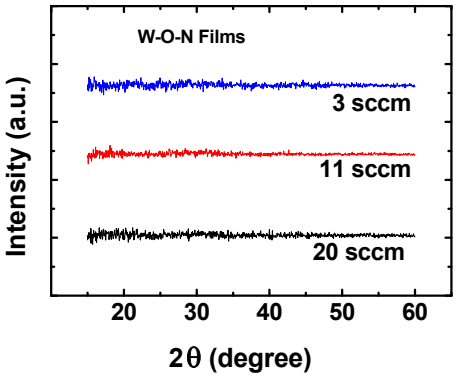

Fig. 1. X-ray diffraction patterns of representative W-O-N films deposited at various nitrogen gas flow rates. The absence of peaks is due to the amorphous nature of the W-O-N films.

amorphous nature of the W-O-N films. While a detailed discussion of the results and data is reported elsewhere [2], the results are summarized briefly for the benefit of understanding the current work. The lack of additional energy, either by substrate heating (thermal energy) or substrate bias voltage (electrical energy), is the main reason for the amorphous character of the W-O-N films under variable gas flow rates. This is in agreement with earlier reports, where an amorphous structure is noted for several of W-oxide or W-Ti mixed oxide thin films [2,9]. Scanning electron microscopy (SEM) images of W-O-N films deposited under variable nitrogen gas flow rate are shown in Fig. 2. The SEM images show a smooth featureless characteristic morphology, indicating a lack of particulates on the film surface. Given the absence of diffraction peaks in GIXRD patterns and the lack of nano-particles in the high resolution SEM images (Fig. 2), it can be concluded that the films are completely amorphous. The cross-sectional SEM images of W-O-N interfaces with Si substrate for W-O-N films deposited at representative nitrogen flow rates are shown in Fig. 3. The W-O-N film and Si-substrate regions are as indicated in Fig. 3. The cross-

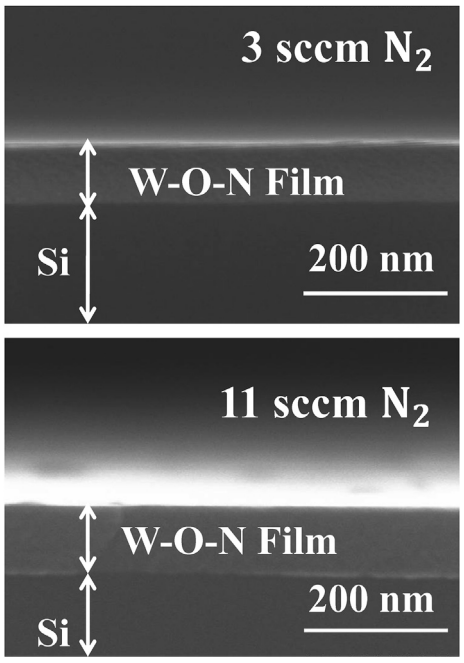

Fig. 3. Cross-sectional SEM images of representative W-O-N films.

sectional SEM images indicate that there is no significant reaction or Si-oxide formation at the interface. Furthermore, the SEM images also provide a means to validate the W-O-N film thickness determined from Ellipsometry modeling (described later below) as they are in excellent agreement with each other.

The spectral dependencies of the ellipsometric parameters, Ψ (azimuth) and Δ (phase change), obtained for W-O-N films grown under variable nitrogen content are shown in Fig. 4. SE measures the relative changes in the amplitude and phase of the linearly polarized white light source upon oblique reflection from the sample surface. The experimental SE parameters, Ψ and Δ, are

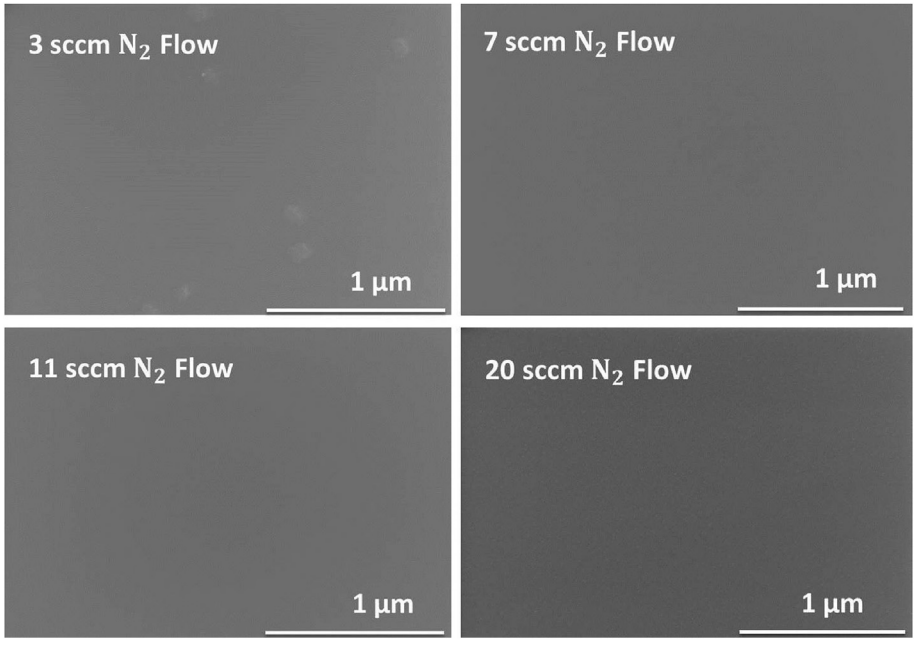

Fig. 2. SEM data of W-O-N films deposited at variable nitrogen gas flow rates. The images indicate a smooth, featureless morphology.

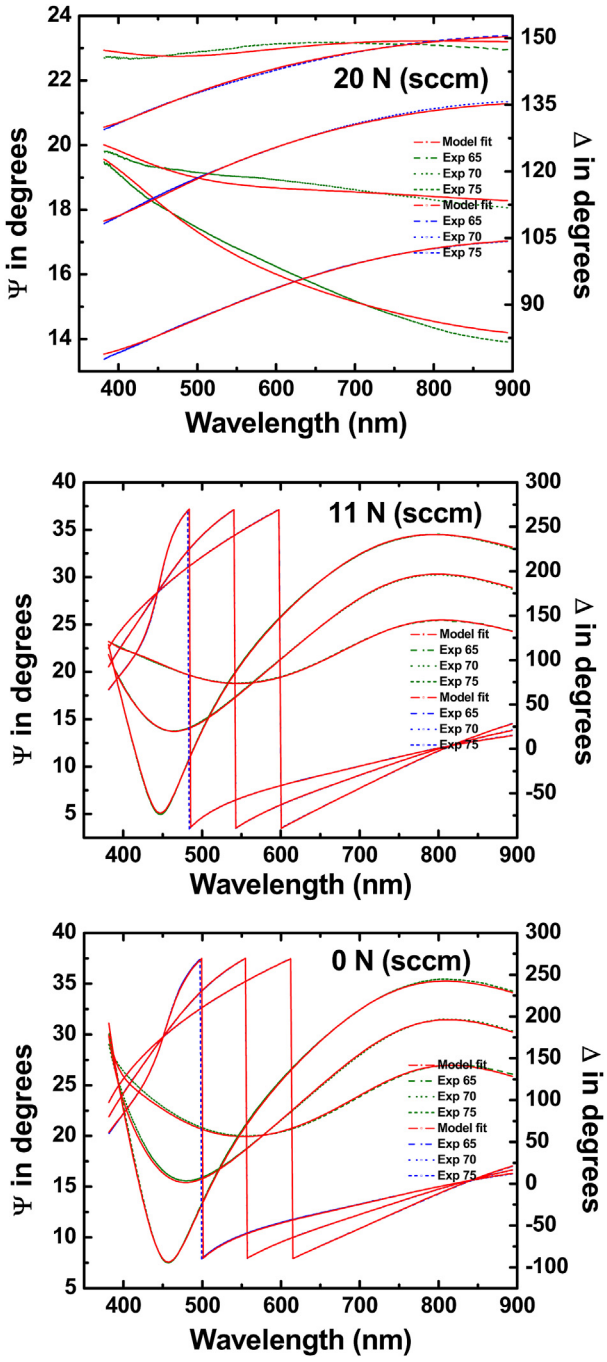

Fig. 4. The spectral dependencies of Ψ and Δ for W-O-N films deposited at various nitrogen flow rates. The experimental data obtained and modeling curves are shown.

related to the microstructure and optical properties, defined by Refs. [23–25]:

$$\rho = R_p/R_s = \tan \Psi \exp(i\Delta) \quad (1)$$

where R_p and R_s are the complex reflection coefficients of the light polarized parallel and perpendicular to the plane of incidence, respectively. The spectral dependencies of ellipsometric parameters Ψ (azimuth) and Δ (phase change) can be fitted with appropriate models to extract the film thickness and optical constants based on the best fit between experimental and simulated spectra [23,24].

The experimental and simulation data curves obtained for W-O-N films are in good agreement with each other (Fig. 4). The Levenberg-Marquardt regression algorithm was used for minimizing the mean-squared error (MSE) [22,23], where the measured (experimental) and calculated ellipsometry functions (Ψ_{exp}, Ψ_{calc} and Δ_{exp}, Δ_{calc}) were used. MSE values higher than 10 were rejected in the fitting procedure to obtain best possible fits. Extracting meaningful physical and optical parameters from SE requires the construction of an optical model of the sample which generally accounts for a number of distinct layers with individual optical dispersions. Interfaces between these layers are optical boundaries at which light is refracted and reflected according to the Fresnel relations. The optical stack model (Fig. 5) employed in this work to simulate the spectra for the purpose of determining the optical constants of W-O-N material contains, from top, W-O-N film, SiO_2 interface and Si substrate. The surface and interface roughness were also considered in order to accurately fit the experimental data. A Tauc–Lorentz (TL) model was used to fit the raw ellipsometry data, and the resulting empirical parameterization is based on the Tauc expression for the imaginary part (ε_2) of the dielectric function [26]. For a single transition, the complex dielectric function ε_2 is defined as [23,26]:

$$\varepsilon_2(E) = \frac{A_L E_0 C (E - E_g)^2}{\left(E^2 - E_0^2\right)^2 + C^2 E^2} \cdot \frac{1}{E} \quad (2)$$

where E_0 is the resonance energy, E_g represents band gap energy, E photon energy, and A_L, C are the amplitude and broadening coefficient of ε_2 peak, respectively, The aforementioned model allowed for the determination of *n* and *k* as well as thickness. Note that the real and imaginary parts of the dielectric function are related to *n* and *k* as: $\varepsilon_1 = n^2 - k^2$; $\varepsilon_2 = 2nk$.

The dispersion profiles of both *n* and *k* are shown in Figs. 6 and 7, respectively. The data shown are for W-O-N films deposited under variable nitrogen content. The *k*-values show a distinct behavior for the samples with increasing nitrogen content during deposition. The W-O-N films deposited at nitrogen gas flow rates ≤9 sccm exhibit more or less similar trend as shown in Fig. 6a. It is evident that '*k*' values are low and very close to zero in most part of the spectrum (Fig. 6a) which indicate very low optical losses due to absorption. The sharp increase in '*k*' at short wavelengths is due to the fundamental absorption across the band gap. An understanding of the quality of W-O-N films can also be derived from the dispersion profiles of $k(\lambda)$. Specifically, the curves (Fig. 6a) indicate that the *k* value of the samples is almost zero in the visible and near infrared spectral regions, while for photon energies towards ultraviolet region, '*k*' increases sharply. Strong absorption with no

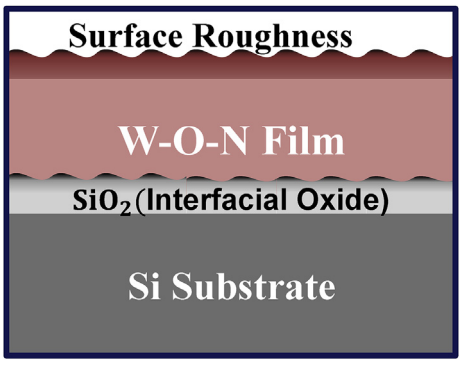

Fig. 5. Stack model of the sample constructed for ellipsometry data analysis.

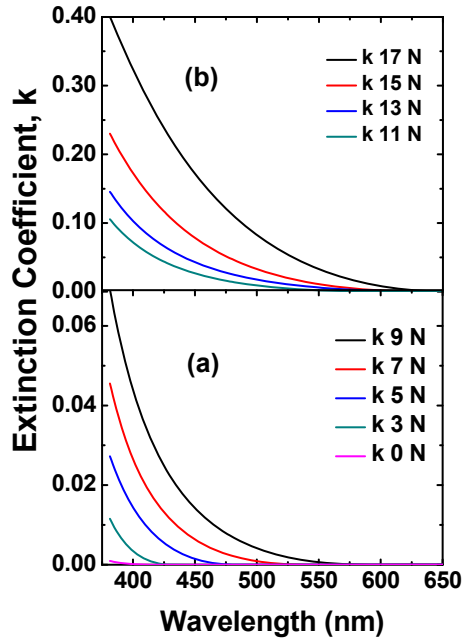

Fig. 6. The spectral dependence of k for W-O-N films deposited at various nitrogen flow rates. (a) k-dispersion curves of samples deposited at a nitrogen flow rate <9 sccm; (b) k-dispersion curves of samples deposited at a nitrogen flow rate ≥9 sccm.

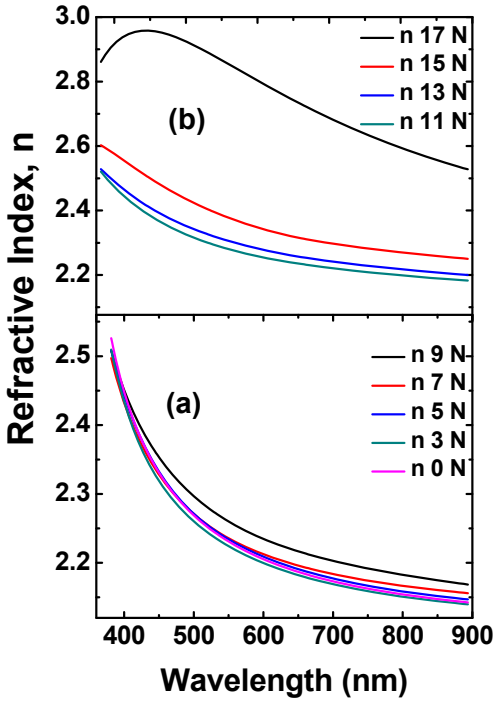

Fig. 7. The spectral dependence of n for W-O-N films deposited at various nitrogen flow rates. (a) n-dispersion curves of samples deposited at a nitrogen flow rate <9 sccm; (b) n-dispersion curves of samples deposited at a nitrogen flow rate ≥9 sccm.

weak shoulders or tailing behavior for the W-O-N films without any nitrogen in the reactive gas mixture can be attributed to the typical oxide (insulating) behavior with very high transparency [2,25]. A remarkable change in $k(\lambda)$ profiles can be noted for W-O-N films deposited at higher nitrogen gas flow rates (>9 sccm). Evidently, incorporation of nitrogen above the threshold of 9 sccm has a significant effect on the spectral dispersion of k. A progressive shift of $k(\lambda)$ profiles to higher values with increasing nitrogen gas flow rate can be seen in Fig. 6b. This transformation of $k(\lambda)$ profiles is attributed to the electronic structure change, where the insulating oxide phase is transforming to semiconducting oxynitride phase. At the maximum nitrogen gas flow rate (17 sccm), W-O-N films exhibit a completely different $k(\lambda)$ profile with trend and values typical to more metallic materials. This is a clear indication of decreased levels of oxygen as well as nitrogen-incorporation induced changes in the optical behavior of W-O-N films.

The $n(\lambda)$ profiles (Fig. 7) of W-O-N films indicate a sensitivity to nitrogen and oxygen gas flow rates, as noted in $k(\lambda)$ profiles. The n dispersion curves also indicate a sharp increase at shorter wavelengths related to the fundamental absorption of energy across the band gap. A gradual positive shift of the n profiles with increasing nitrogen content is also shown within Fig. 7, analogous to the shifts demonstrated by k in Fig. 6. Similar to $k(\lambda)$ profiles, the $n(\lambda)$ profiles can also be conveniently grouped into two different sets corresponding to nitrogen gas flow rates above and below 9 sccm. The n values obtained (Fig. 7a) in this work for W-O-N films without any nitrogen in reactive gas mixture are close to that of bulk WO_3, indicating that the films are comprised of a W-oxide phase with stoichiometry close to WO_3 [2]. The optical constants of the W-O-N films, deposited at nitrogen gas flow rates at ≤9 sccm, indicate more or less similar behavior and magnitude. An increase in magnitude, as well as positive shift in the n-profiles, can also be noted for W-O-N films deposited at higher (>9 sccm) nitrogen flow rates (Fig. 7b). It can be seen that the n-profiles and magnitude for the W-O-N films deposited at the highest nitrogen content (17 sccm) are quite different compared to those deposited at lower nitrogen gas flow rates. Most notable are the elevated values of n for samples deposited at the 17 sccm N_2. Progressive increases in both n and k values with increasing nitrogen content indicate a potential compositional-change induced electronic structure transformation in the W-O-N films. It should be noted that the n value is directly related to the material density and molecular polarizability. Therefore, the increasing n-values for W-O-N films with increasing nitrogen flow rate ratio must be a result of changes in the material density as well as changes in molecular polarizability, or a combined effect thereof [2,25].

The optical transmittance spectra of W-O-N films deposited at variable nitrogen gas flow rate are shown in Fig. 8. In general, relatively high transparency of the W-O-N films is evident in the measured spectral region, except where the incident radiation is absorbed across the band gap (E_g). It is also evident that the spectral

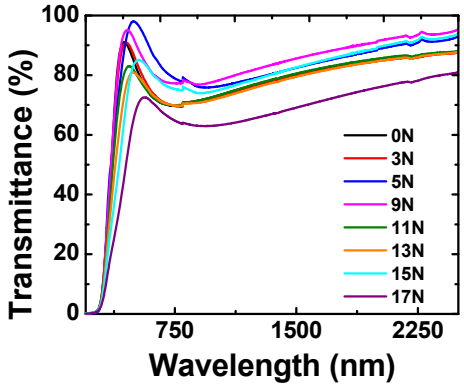

Fig. 8. Spectral transmittance characteristics of W-O-N films deposited at variable nitrogen gas flow rates. The transparent nature of the films is evident from these curves.

transmission curves undergo incremental changes as a result of increasing the nitrogen content. Most notable is the red-shift in spectral absorption coupled with decreased spectral transmittance for W-O-N films with increasing nitrogen gas flow rate. This observations indicates a significant change in the electronic structure of the W-O-N films as a function of nitrogen content. Furthermore, since ellipsometry analyses were performed over a limited spectral region, the transmittance data of W-O-N films provide a means to validate the model employed and optical quality the W-O-N films determined using the ellipsometry functions. The E_g values were determined using the optical absorption coefficient [2] calculated from transmittance curves and are listed in Table 1.

Further analysis of the optical dispersion, and the correlation between optical parameters and material characteristics of W-O-N films, has been made by considering the evolution of *n*-profiles as a function of nitrogen content. For W-O-N films with varying composition, the dispersion of refractive index is simulated with Wemple and DiDomenico (W-D) single oscillator dispersion model [27,28], which is proven to be valuable and applicable to several single-bond simple oxides as well as a number of multiband, complex oxides with multiple cations assuming different coordination numbers [27–32]. In the W-D dispersion model, the refractive index can be expressed as:

$$n^2 - 1 = \frac{E_0 E_d}{\left(E_0^2 - E^2\right)} \tag{3}$$

where E ($=\hbar\omega$) is the incident photon energy, E_0 is the oscillator energy and E_d is the dispersion energy [27,28]. Plots of $(n^2-1)^{-1}$ vs. E^2 for W-O-N films deposited at various nitrogen flow rates are shown in Fig. 9. The linear relationship indicating the validity of W-D model for the *n*-dispersion of W-O-N films is evident from these plots. E_0 and E_d were calculated using linear plots of $(n^2-1)^{-1}$ vs. E^2 by determining the slope and y-intercept. The resulting parameters of the model are presented in Table 1. It is evident that both E_0 and E_d are dependent on the nitrogen gas flow rate which is an indicative of chemical changes in W-O-N films strongly influence their optical behavior. The data from Table 1 excludes the data from the refractive index at a flow of 17 sccm since this data did not fit the model properly to allow an accurate calculation of the energies. Along with the oscillator energy and dispersion energy, band gap (E_g) was also approximated using the relation proposed by Tanaka [32]. These calculated values are comparable to those determined from UV-VIS-NIR spectroscopy and ellipsometry measurements. Furthermore, the decreasing trend of band gap as a function of nitrogen flow is also confirmed again with the data presented in Table 1, a comparison of the data is presented in Fig. 10. The overall decreasing trend is indicated by a solid line in Fig. 10.

The significance of E_0 and E_d and the trend observed for W-O-N films as a function of nitrogen content can be understood as follows. E_d is the measure of intensity of interband optical transitions

Table 1
Optical properties determined from the Wemple and DiDomenico (WDD) dispersion modeling of the refractive index data.

Nitrogen flow (sccm)	UV E_g (eV)	WDD E_g (eV)	E_0 (eV)	E_d (eV)
0	2.90	3.25	6.50	22.45
3	2.89	3.24	6.48	22.24
5	2.88	3.04	6.07	20.91
7	2.84	3.05	6.10	21.18
9	2.67	2.86	5.72	19.99
11	2.65	2.78	5.56	19.85
13	2.56	2.58	5.17	18.40
15	2.30	2.36	4.71	17.48

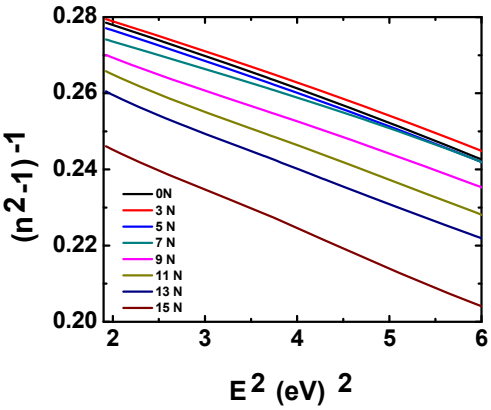

Fig. 9. Plots of $(n^2-1)^{-1}$ vs. E^2 for W-O-N films. The data fitting was made using the Wemple and DiDomenico (WDD) dispersion model. As indicated by the arrow there is a clear effect on the plots as the flow of nitrogen increases.

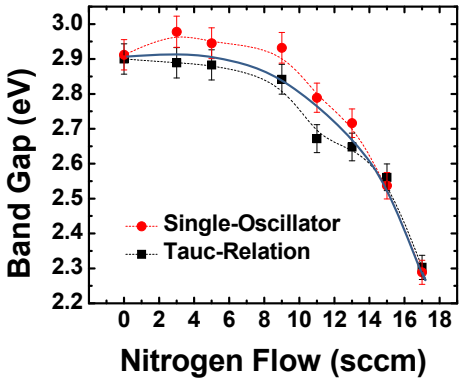

Fig. 10. Comparison of E_g values determined from different methods. The solid line is a guide to the eye to understand the decreasing trend of E_g values with increasing nitrogen content in the W-O-N films.

[27,28]. E_d is an important optical parameter for optical or electro-optic materials and quite useful in designing devices for optical communication and for spectral dispersion applications. On the other hand, single-oscillator energy E0 simulates all the electronic excitations involved [27,28]. According to W-D model, the dispersion energy is a characteristic parameter that depends on the charge distribution, which would be closely related to chemical bonding of the material [27–32]. E_d is, therefore, related to the materials' physical parameters through the following empirical relationship:

$$E_d = \beta N_c Z_a N_e \tag{4}$$

where N_c is the effective coordination number of the cation nearest neighbors to the anion, Z_a is the formal chemical valence of the anion, N_e is the effective number of valence electrons per anion and β is a two-valued constant with the either an ionic or a covalent value. As documented widely in the literature, $\beta = 0.26$ for ionic compounds and $\beta = 0.37$ for covalent compounds [29–31]. Thus, all the material characteristics (N_c, N_e and Z_a) of W-O-N films were determined considering the chemical composition of the films (oxygen to nitrogen ratio) and taking $\beta = 0.26$. It is seen that the N_c, N_e and Z_a values are sensitive to the nitrogen content in the reactive gas mixture and the final chemical composition of the resulting W-O-N films. While N_c and N_e values decrease with increasing nitrogen content, Z_a values increase with increasing nitrogen content.

The variation of N_e and Z_a with nitrogen flow rate is shown in Fig. 11. Note that these two parameters are directly connected to the chemical bonding involved and the extent of charge transfer to form such chemical bond. Therefore, N_e and Z_a values determined using W-D model and their variation with nitrogen flow rate have important implications and provide insights into the underlying chemistry and physics of electronic structure changes in W-O-N films. The decreasing tendency of N_e can be understood as follows. According to Pauling's electronegativity rules, the ionic character (ionicity) of a chemical bond between two atoms is due to the difference in electronegativity values of those two atoms involved. The metal-oxygen (M-O) bonds usually have a higher ionicity than that of metal-nitrogen (M-N) bonds due to the fact that the electronegativity of oxygen (3.5) is higher than that of nitrogen (3.0). Therefore, the M-O bonds involve a higher level of charge transfer than the M-N bonds. A direct consequence of this charge transfer difference between M-O and M-N bonds to the present study is the overall decrease in ionic character with effective nitrogen incorporation resulting in W-O-N oxynitride films [33]. However, the net increase in Z_a or decrease in N_e is not effective until the critical nitrogen flow rate since the material is predominantly W-oxide with essentially no contribution from W-N bonds. At, or above, the critical nitrogen flow rate, the W-N bonds will increase relative to W-O bonds in the W-O-N films. Thus, while Z_a increases due to increase in nitrogen content in the W-O-N films, the overall charge redistribution results in decreasing N_e values. As a consequence, the E_0 and E_g values also decrease. However, the observed decrease in E_0 and E_g values can also be explained from a different perspective based on electronic states mixing. E_g and E_0 decrease with increasing nitrogen is due the narrowing of the band gap due to the existence of both the N 2p states with O 2p states simultaneously [33–36]. The band gap energy (E_g) value corresponds to energy of electronic transitions from the top of valence band to the conduction band [2,4,6,7,10,11,37–39]. The valence and conduction bands in WO_3 are formed by the O 2p and W 3d states, respectively. When nitrogen is introduced into the WO_3 lattice, since N 2p states are energetically close and favorable to O 2p states, the N 2p states tend to intermix with O 2p states. As a result, the valence band in W-O-N is now consists of both O 2p states and N 2p states while the conduction band is still with empty W 3d states. Thus the nitrogen incorporation into tungsten oxide results in the expansion of the valence band since N 2p states are occupied above O 2p states [33,34]. The consequence of this phenomenon is a decrease in band gap values corresponding to the amount of nitrogen incorporated into the films. No significant changes seen in the initial set of W-O-N films, due to the fact that the nitrogen incorporation into WO_3 is not effective and the valence band is essentially consists of O 2p states. When an increase in nitrogen content is seen above 9 sccm, a variably lower band gap is observed in this work. With the addition of N 2p states to the valence band, so that both N 2p and O 2p states exist, a significant narrowing of band gap occurs due to the expansion of the valence band. Ti-O-N and Zn-O-N films have shown similar behavior with comparable band gap values [33–36].

The direct evidence for the aforementioned chemical changes and relative increase or decrease of W-N and W-O bonds is provided by the chemical analyses made using X-ray photoelectron spectroscopy (XPS) and Rutherford backscattering spectrometry (RBS) analyses on the W-O-N films. While the specific details of XPS and RBS experiments and preliminary data are reported elsewhere [2], a summary of the chemical composition and relative changes in nitrogen and oxygen concentration is presented in Fig. 12. The lines and arrows are provided to guide the eye. It is evident that the film chemical composition i.e., the relative content of nitrogen versus oxygen, changes with increasing nitrogen flow rate. The W-O-N films grown without any nitrogen correspond to stoichiometric WO_3. The visual examination of these films revealed a bluish color, which matches with the well-known, fully stoichiometric tungsten oxide. Similarly, the W-O-N films grown without any oxygen correspond to stoichiometric WN_2. The visual appearance of these films is brownish, metallic in nature. Thus, this end member also has a clear distinction with a brown color of electrically conductive tungsten nitride. Both XPS and RBS analyses indicate that the nitrogen incorporation is not very effective for the set of samples deposited under nitrogen flow rates $\leq$9 sccm, at which point an increase in the nitrogen concentration is significant leading to the formation of W-O-N films. Incorporation of nitrogen content in the films accompanied by a decrease in oxygen content. The estimated composition, at 9 sccm of nitrogen, from RBS data is $WO_{2.60}N_{0.40}$. Further increases in nitrogen content, and decreases in oxygen, are noted in the W-O-N films for nitrogen flow rates $\geq$9 sccm. The chemical analyses confirm that the chemical composition and the oxygen to nitrogen ratio in the W-O-N films progress through the sequence:

$$WO_3 \rightarrow WO_{2.60}N_{0.40} \rightarrow WO_{2.48}N_{0.52} \rightarrow WO_{2.20}N_{0.80} \rightarrow WN_2$$

Mechanical characteristics of the W-O-N films were considered anticipating that the aforementioned chemical changes will also reflect changes in the surface hardness and Young's modulus. The results obtained from nano-indentation measurements are shown in Fig. 13, where variation in the hardness and Young's Modulus with nitrogen flow rate is presented. Well known Oliver and Pharr method has been employed to calculate the mechanical characteristics; known geometry and mechanical properties of the indenter were used in the calculation. Both the hardness and

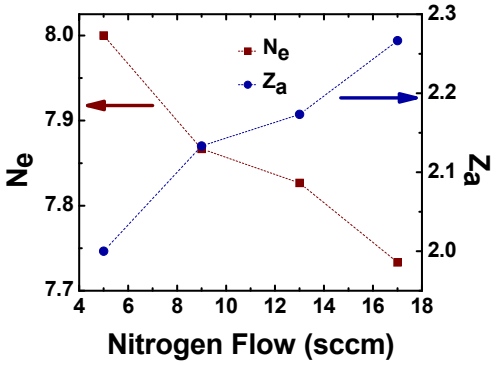

Fig. 11. The variation of N_e and Z_a with nitrogen flow rate in W-O-N films.

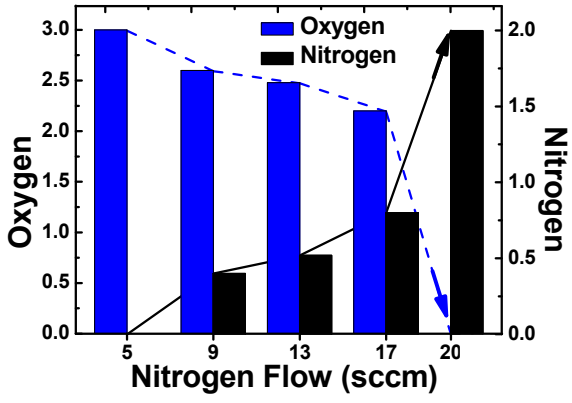

Fig. 12. Evolution of oxygen and nitrogen content in W-O-N films with reactive nitrogen gas flow rate.

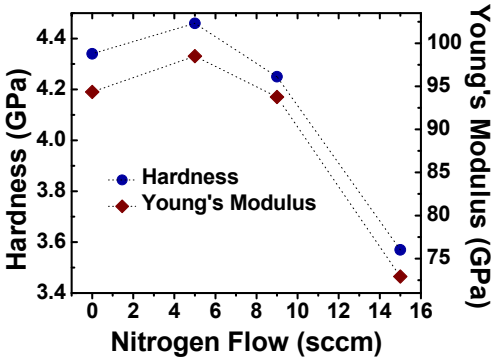

Fig. 13. Mechanical properties, hardness and Young's modulus, of W-O-N films as measured by nano-indentation tests.

Young's modulus follow the same trend with increasing nitrogen flow rate. It is evident that the hardness initially increases with increasing nitrogen gas flow rate and attains a maximum of ~4.5 GPa at 5 sccm. Similarly, the Young's modulus of the W-O-N films also increases with increasing nitrogen flow rates and attains a maximum of 98.5 GPa. However, further increases in nitrogen flow rate beyond 5 sccm result in a decrease of the hardness and Young's modulus values. The hardness and Young's modulus reach minimum values of ~3.6 GPa and 72.9 GPa, respectively, at a nitrogen flow rate of 15 sccm. Note that the values determined for W-O-N films in this work are significantly lower compared to those values found in the literature, where the range reported is 15–30 GPa. The low values obtained in this work can be attributed to the amorphous structure of the films and mechanical integrity of the substrate material [40–42]. For the W-O-N films produced with variable nitrogen content, as reported previously elsewhere [2], the GIXRD analyses indicate that the W-O-N films were amorphous in the entire range of nitrogen flow rates. The other contributing factor to the lower values observed is the fact that the W-O-N films were grown on silicon substrates rather than substrates made of steel or superalloy [43]. As reported by several authors and widely accepted in the literature, mechanical properties decrease when the film exhibits an amorphous structure and also when the internal stresses in the films become relaxed [41,42,44]. For instance, as demonstrated by Dubey et al., the magnitudes of hardness and Young's modulus are directly related to the structure [44]. In their work on binary and ternary nitrides, it was shown that that the hardness and elastic modulus decrease when the film becomes amorphous due to the lack of hindrance to dislocation movements that grain growth tends to promote [44]. The observed decrease in hardness and Young's modulus for W-O-N films can, therefore, be attributed to the high degree of structural disorder correlated to increased nitrogen flow. The degree of such disorder may increase with increasing nitrogen due to the competitive nature of nitrogen and oxygen atoms during reactive deposition. This is also evident from optical analyses, which indicate that the disorder energy increases with increasing nitrogen gas flow rate. Shen et al. reported that, with increasing oxygen concentration, there will be a competing tendency between nitrogen and oxygen atoms and the relaxation of internal compressive stresses occur for either oxygen atoms taking the place of nitrogen atoms or nitrogen atoms substituting for oxygen within the lattice [45,46]. Furthermore, it has been demonstrated for nitrides that nitrogen reduces the mobility of tungsten, or other metallic particles, or nitrogen can even act as a nucleation site for defects [44,47]. These factors, as well as an increase of oxygen content seen in the same range as the lower values for the mechanical properties (Fig. 13), lead to an increasingly amorphous structure, lowering hardness and Young's modulus values [48]. Thus, the decreasing trend observed (Fig. 12) in our W-O-N films is commonly seen in samples where oxygen incorporation and nitrogen content contributes to the relaxation of internal stresses [41,42]. The results are in good agreement with those reported by Parreira et al. [41] and Khamseh [41,42].

Finally, optical properties were considered to model the physical density of the W-O-N films not only to account for the observed optical properties but also to account for the significance of the optical properties. The density of the W-O-N films was calculated using the Lorentz-Lorentz relation [9,25]:

$$\frac{\rho_f}{\rho_b} = \left[\frac{\left(n_f - 1\right)^2}{\left(n_f + 1\right)^2} \cdot \frac{(n_b + 1)^2}{(n_b - 1)^2}\right], \tag{5}$$

where ρ_f and ρ_b are the densities of the deposited films and bulk material, respectively, n_f is the refractive index for the W-O-N film and n_b is the refractive index for bulk W-O-N. The rule of mixtures was employed to estimate the bulk density. Using the chemical composition found through XPS and RBS analyses, the density and index of refraction (n_b) values for the bulk materials were calculated using the fraction of W-O and W-N bonds within WO_xN_y. The fractions of each bond was then used to estimate the new value of the bulk material by assuming the index of refraction for bulk WO_3 and WN, at ~630 nm, to be 2.0 [48] and 3.8 [49,50], respectively, and their bulk densities to be 7.16 g/cm^3 [51] and 17.7 g/cm^3 [52,53], respectively. The measured values n at ~630 nm from SE for W-O-N films were then used to calculate the approximate values of the density for the deposited W-O-N thin films as a function of nitrogen flow rate. The results of the analysis are presented in Fig. 14, where it can be seen that there is a direct correlation between the measured index of refraction and density of the films. Increases in both the index of refraction and the density of the W-O-N film increases are a direct consequence of growing nitrogen content in the films proportional to the nitrogen gas flow rate. While the quantitative analysis is not attempted, Mohamad and Shaaban have also reported that the index of refraction increase in W-O-N films could be due to augmentation of the film density [54]. Thus, the density increase and molecular polarizability changes due to relative changes in W-N and W-O bonds account for the observed changes in the optical parameters namely, the index of refraction, absorption coefficient and dispersion energy parameters of W-O-N films as a function of nitrogen gas flow rate. The n and k changes are also correlated to the electronic structure changes in W-O-N films

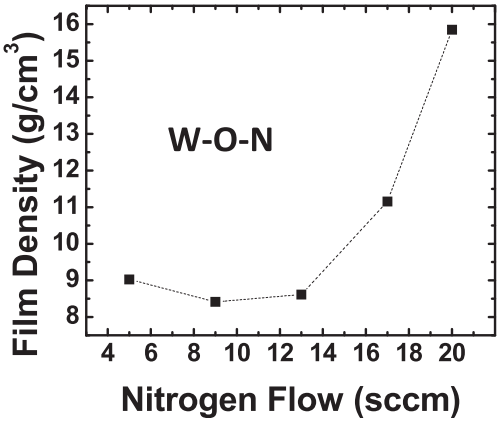

Fig. 14. Density variation of W-O-N films with nitrogen flow rate. It is evident that the film density increase with increasing nitrogen gas flow rate.

as a function of increasing nitrogen content.

4. Conclusions

Amorphous W-O-N thin films were fabricated using DC sputter-deposition by varying nitrogen gas flow rate in the range of 0–20 sccm while keeping the total gas flow constant at 40 sccm. The index of refraction (n) and extinction coefficient (k) of W-O-N films were shown to be highly sensitive to the gas mixtures within the deposition chamber, increasing alongside nitrogen content. Changes in the electronic structure, in the sequence of W-oxide (~3 eV) → W-O-N oxynitride semiconductor (2 eV) → N-rich W-O-N semi-metal (<2 eV) → WN_2 type transition, were evident in dispersion profiles of n and k for W-O-N films with increasing nitrogen gas flow rate from 0 to 20 sccm. The evolution of the chemical composition, and the formation of both W-N and W-O bonds in the W-O-N films, affects both the optical and mechanical properties of the films. The optical band gap, determined from the WDD model, decreases from the highest value at E_g ~ 3.0 eV, in samples grown with no nitrogen flow, to ~2.1 eV as the nitrogen flow increases. The trend observed for the dispersion energy parameters, N_e and Z_e values determined from WDD model, correlate with the chemical structure changes in W-O-N films as consequence of the changing ionicity due to an increase of W-N bonds and the intermixing of N 2p and O 2p states in the valence band. The correlation between the nitrogen content and optical constants, along with associated dispersion energy parameters, demonstrates that tailoring the optical behavior of W-O-N films for selective applications can be readily achieved by tuning the nitrogen content and chemical composition.

Acknowledgements

Authors at the University of Texas at El Paso acknowledge, with pleasure, support from the National Science Foundation (NSF) with NSF-PREM grant # DMR-1205302. Authors are thankful to the Dr. K. Hossain at Amethyst Research Inc., Ardmore, Oklahoma for helpful discussions and RBS measurements on some of our samples. One of us (Adbeel Moreno-Tarango) is thankful for the internship opportunity by the US Air Force through the Collaborative Research Program to perform research work at the Materials and Manufacturing Directorate, Wright Patterson Air Force Base, Ohio.

References

[1] C.G. Granqvist, Handbook of Inorganic Electrochromic Materials, Elsevier, New York, 1995.
[2] O.R. Nunez, A.J. Moreno Tarango, N.R. Murphy, L.C. Phinney, K. Hossain, C.V. Ramana, Physical characterization of sputter-deposited amorphous tungsten oxynitride thin films, Thin Solid Films 596 (2015) 160–166.
[3] Y. Xin, H. Zhou, X. Ni, Y. Pan, X. Zhang, J. Yun Zheng, S. Bao, P. Jin, The optical properties of low infrared transmittance WO_{3-x} nanocrystal thin films prepared by DC magnetron sputtering under different oxygen ratios, RSC Adv. 5 (2015) 57757–57763.
[4] W. Li, P. Da, Y. Zhang, Y. Wang, X. Lin, X. Gong, WO_3 nano flakes for enhanced photoelectrochemical conversion, ACS Nano 8 (2014) 11770–11777.
[5] M.V. Limaye, J.S. Chen, S.B. Singh, Y.C. Shao, Y.F. Wang, C.W. Pao, H.M. Tsai, J.F. Lee, H.J. Lin, J.W. Chiou, M.C. Yang, W.T. Wu, J.S. Chen, J.J. Wu, M.H. Tsai, W.F. Pong, Correlation between electrochromism and electronic structures of tungsten oxide films, RSC Adv. 4 (2014) 5036–5045.
[6] A. Karuppasamy, A. Subrahmanyam, Studies on electrochromic smart windows based on titanium doped WO_3 thin films, Thin Solid Films 516 (2007) 175–178.
[7] X. Sun, Z. Liu, H. Cao, Electrochromic properties of N-doped tungsten oxide thin films prepared by reactive DC-pulsed sputtering, Thin Solid Films 519 (2011) 3032–3036.
[8] S. Adhikari, D. Sarkar, Hydrothermal synthesis and electrochromism of WO_3 nanocuboids, RSC Adv. 4 (2014) 20145–20153.
[9] C.V. Ramana, G. Baghmar, E.J. Rubio, M.J. Hernandez, Optical constants of amorphous, transparent titanium-doped tungsten oxide thin films, ACS Appl. Mater. Interfaces 5 (2013) 4659–4666.
[10] S.K. Gullapalli, R.S. Vemuri, C.V. Ramana, Structural transformation induced changes in the optical properties of nanocrystalline tungsten oxide thin films, Appl. Phys. Lett. 96 (2010) 1–4.
[11] S.H. Mohamed, A. Anders, Structural, optical, and electrical properties of WOx(Ny) films deposited by reactive dual magnetron sputtering, Surf. Coatings Technol. 201 (2006) 2977–2983.
[12] B. Marsen, E.L. Miller, D. Paluselli, R.E. Rocheleau, Progress in sputtered tungsten trioxide for photoelectrode applications, Int. J. Hydrogen Energy 32 (2007) 3110–3115.
[13] D. Paluselli, B. Marsen, E.L. Miller, R.E. Rocheleau, Nitrogen doping of reactively sputtered tungsten oxide films, Electrochem. Solid State Lett. 8 (2005) G301–G303.
[14] Y. Sun, C.J. Murphy, K.R. Reyes-Gil, E.A. Reyes-Garcia, J.M. Thornton, N.A. Morris, D. Raftery, Photoelectrochemical and structural characterization of carbon-doped WO_3 films prepared via spray pyrolysis, Int. J. Hydrogen Energy 34 (2009) 8476–8484.
[15] S.H. Cheung, P. Nachimuthu, A.G. Joly, M.H. Engelhard, M.K. Bowman, S.A. Chambers, N incorporation and electronic structure in N-doped TiO_2(110) rutile, Surf. Sci. 601 (2005) 1754–1762.
[16] M. Batzill, E.H. Morales, U. Diebold, Influence of nitrogen doping on the defect formation and surface properties of TiO_2 rutile and anatase, Phys. Rev. Lett. 96 (2006) 026103.
[17] S.A. Chambers, Ferromagnetism in doped thin-film oxide and nitride semiconductors and dielectrics, Surf. Sci. Rep. 61 (2006) 345–381.
[18] K.J. Lethy, S. Potdar, V.P. Mahadevan Pillai, V. Ganesan, Transparent and low resistive nanostructured laser ablated tungsten oxide thin films by nitrogen doping: II. Substrate temperature, J. Phys. D. Appl. Phys. 42 (2009) 095412.
[19] L. Gomathi Devi, R. Kavitha, Review on modified N–TiO_2 for green energy applications under UV/visible light: selected results and reaction mechanisms, RSC Adv. 4 (2014) 28265–28299.
[20] X. Zhang, X. Cui, Facile synthesis of flowery N-doped titanates with enhanced adsorption and photocatalytic performances, RSC Adv. 4 (2014) 60907–60913.
[21] X. Sha, F. Tian, D. Li, D. Duan, B. Chu, Y. Liu, B. Liu, T. Cui, Ab initio study on the stability of N-doped ZnO under high pressure, RSC Adv. 5 (2015) 16774–16779.
[22] J. A. Woollam Co., Inc., Guide to Using WVASE32 Spectroscopic Ellipsometry Data Acquisition and Analysis Software (2008).
[23] G.E. Jellison Jr., Spectroscopic ellipsometry data analysis: measured versus calculated quantities, Thin Solid Films 313–314 (1998) 33–39.
[24] H. Fujiwara, Spectroscopic Ellipsometry: Principles and Applications, John Wiley & Sons Inc., 2007.
[25] M. Vargas, E.J. Rubio, A. Gutierrez, C.V. Ramana, Spectroscopic ellipsometry determination of the optical constants of titanium doped tungsten oxide thing films, J. Appl. Phys. 115 (2014) 1335111.
[26] J. Tauc, R. Grigorovici, A. Vancu, Optical properties and electronic structure of amorphous germanium, Phys. Stat. Sol. B 15 (1966) 627–637.
[27] S.H. Wemple, M. DiDomenico, Behavior of the electronic dielectric constant in covalent and ionic materials, Phys. Rev. B 3 (1971) 1338–1351.
[28] S.H. Wemple, Optical oscillator strengths and excitation energies in solids, liquids, and molecules, J. Chem. Phys. 67 (1977) 2151–2166.
[29] O. Medenbach, D. Dettmar, R.D. Shannon, R.X. Fischer, W.M. Yen, Refractive index and optical dispersion of rare earth oxides using a small-prism technique, J. Opt. A Pure Appl. Opt. 3 (2001) 174–177.
[30] M. Caglar, S. Ilican, Y. Calgan, Y. Sahin, F. Yakuphanoglu, D. Hur, A spectroelectrochemical study on single-oscillator model and optical constants of sulfonated polyaniline film, Spectrochim. Acta A 71 (2008) 621–627.
[31] A. Timoumi, H. Bouzouita, B. Rezig, Aust. J. Basic Appl. Sci. 7 (2013) 448–456.
[32] K. Tanaka, Optical properties and photoinduced changes in amorphous As-S films, Thin Solid Films 66 (1980) 271–279.
[33] M. Futsuhara, K. Yoshioka, O. Takai, Optical properties of zing oxynitride thin films, Thin Solid Films 317 (1998) 322–325.
[34] H. Le Dréo, O. Banakh, H. Keppner, P.-A. Steinmann, D. Briand, N.F. de Rooij, Optical, electrical and mechanical properties of the tantalum oxynitride thin films deposited by pulsing reactive gas sputtering, Thin Solid Films 515 (2006) 952–956.
[35] J.H. Hsieh, C.C. Chang, J.S. Cherng, F.Y. Hsu, Optical properties and hydrophilic behaviors of TaO_xN_y thin films with and without rapid thermal annealing, Thin Solid Films 517 (2009) 4711–4714.
[36] X. Yang, C. Li, B. Yang, W. Wang, Y. Qian, Optical properties of titanium oxynitride nanocrystals synthesized via a thermal liquid-solid metathesis reaction, Chem. Phys. Lett. 383 (2004) 502–506.
[37] H. Simchi, B.E. McCandless, T. Meng, W.N. Shafarman, Structural, optical, and surface properties of WO_3 thin films for solar cells, J. Alloys. Compd. 617 (2014) 609–615.
[38] S. Higashimoto, M. Sakiyama, M. Azuma, Photoelectrochemical properties of hybrid WO_3/TiO_2 electrode. Effect of structures of WO_3 on charge separation behavior, Thin Solid Films 503 (2006) 201–206.
[39] A.K. Chawla, S. Singhal, H. Om Gupta, R. Chandra, Influence of nitrogen doping on the sputter-deposited WO_3 films, Thin Solid Films 518 (2009) 1430–1433.
[40] C. Louro, J.C. Oliveira, A. Cavaleiro, Effects of O addition on the thermal behavior of hard W-N sputtered coatings, Vacuum 83 (2009) 1224–1227.
[41] N.M.G. Parreira, N.J.M. Carvalho, F. Vaz, A. Cavaleiro, Mechanical evaluation of unbiased W-O-N coatings deposited by d.c. reactive magnetron sputtering, Surf. Coat. Technol. 200 (2006) 6511–6516.

[42] S. Khamseh, Synthesis and characterization of tungsten oxynitride films deposited by reactive magnetron sputtering, J. Alloys. Compd. 611 (2014) 249–252.
[43] R. Saha, W.D. Nix, Effects of the substrate on the determination of thin film mechanical properties by nanoindentation, Acta Mater. 50 (2002) 23–38.
[44] P. Dubey, V. Arya, S. Srivastava, D. Singh, R. Chandra, Effect of nitrogen flow rate on structural and mechanical properties of Zirconium Tungsten Nitride (Zr-W-N) coatings deposited by magnetron sputtering, Surf. Coat. Technol. 236 (2013) 182–187.
[45] Y.G. Shen, Y.W. Mai, Effect of oxygen on residual stress and structural properties of tungsten nitride films grown by reactive magnetron sputtering, Mater. Sci. Eng. B 76 (2000) 107–115.
[46] Y.G. Shen, Y.W. Mai, Reactively sputtered WO_xN_y films, J. Mater. Res. 15 (2000) 2437–2445.
[47] Y.G. Shen, Y.W. Mai, D.R. McKenzie, Q.C. Zhang, W.D. McFall, W.E. McBride, Composition, residual stress, and structural properties of thin tungsten nitride films deposited by reactive magnetron sputtering, J. Appl. Phys. 88 (2000) 1380–1388.
[48] K. Hong, K. Kim, S. Kim, I. Lee, H. Cho, S. Yoo, H.W. Choi, N.-Y. Lee, Y.-H. Tak, J.-L. Lee, Optical properties of WO_3/Ag/WO_3 multilayer As transparent cathode in top-emitting organic light emitting diodes, J. Phys. Chem. C 115 (2011) 3453–3459.
[49] P. Boher, P. Houdy, P. Kaikati, L.J. Van Ijzendoorn, Radio frequency sputtering of tungsten/tungsten nitride multilayers on GaAs, J. Vac. Sci. Technol. A 8 (1990) 846–850.
[50] J.W. Klaus, S.J. Ferro, S.M. George, Atomically controlled growth of tungsten and tungsten nitride using sequential surface reactions, Appl. Surf. Sci. 162 (2000) 479–491.
[51] T. Polcar, A. Cavaleiro, Structure, mechanical properties and tribology of W–N and W–O coatings, Int. J. Refract. Met. Hard Mater. 28 (2010) 15–22.
[52] Y.G. Shen, Y.W. Mai, Effect of deposition conditions on internal stresses and microstructure of reactively sputtered tungsten nitride film, Surf. Coat. Technol. 127 (2000) 239–246.
[53] D. Mergel, D. Buschendorf, S. Eggert, R. Grammes, B. Samset, Density and refractive index of TiO_2 films prepared by reactive evaporation, Thin Solid Films 371 (2000) 218–224.
[54] S.H. Mohamed, E.R. Shaaban, Investigation of the refractive index and dispersion parameters of tungsten oxynitride thin films, Mater. Chem. Phys. 121 (2010) 249–253.